Composites Communications 27 (2021) 100815

Contents lists available at ScienceDirect

Composites Communications

journal homepage: www.elsevier.com/locate/coco

Plasticization stretching strategy towards high strength nacre-like graphene-based composites

Cheng Sun, Peng Li, Haoguang Huang, Xin Ming, Mincheng Yang, Yingjun Liu *, Chao Gao **

MOE Key Laboratory of Macromolecular Synthesis and Functionalization, Department of Polymer Science and Engineering, Key Laboratory of Adsorption and Separation Materials & Technologies of Zhejiang Province, Zhejiang University, 38 Zheda Road, Hangzhou, 310027, PR China

ARTICLE INFO

Keywords:
Graphene
Wrinkles
Plasticization stretching
Composites

ABSTRACT

Introducing graphene into polymers is a common method to prepare nacre-like functional composites with enhanced mechanical strength and conductive properties. However, the soft nature of graphene sheets makes it easy to form chaotic wrinkles and degrade the mechanical performance of the composites by hindering interlayer stress transfer. Here, we use a simple plasticization and stretching method to flatten the sheet wrinkles and obtain a highly oriented and crystalline graphene-based nacre-like composite film. The composite film shows excellent mechanical properties (tensile strength of 709.2 MPa, toughness of 11.1 MJ m^{-3}), as well as high electrical conductivity of 7671 S m^{-1}, which are much higher than those of as-prepared films without plasticization and stretching. This low cost and facile method opens an avenue to prepare graphene and other 2D nanosheet based composites with enhanced performance.

1. Introduction

Natural materials such as nacre possess superior mechanical properties to defend external shocks. This outstanding performance can be attributed to the rich interface interactions in the building block structure [1,2]. The nacre-like structure sheds light on the construction of graphene-based composites materials for further increase in mechanical properties. Graphene is considered as an ideal reinforcement filler for structural and functional composite materials owing to the superior mechanical strength (130 GPa) and excellent electrical/thermal conductivities (10^8 S m^{-1}, 5300 W $m^{-1}\cdot K^{-1}$) [3,4]. Versatile strategies have been proposed to improve the overall performance of graphene-based composites. For example, Cheng et al. investigated synergistic interfacial interaction mechanism to strengthen the graphene-based materials by introducing ionic bonding, hydrogen bonding, and covalent bonding [5,6]. Liu and Xu grafted polyacrylonitrile uniformly onto the surface of graphene oxide (GO) and obtained a nacre-like structured graphene fiber with a tensile strength of 452 MPa [7].

However, the wrinkles in the nacre-like composites usually severely degrade the mechanical performance of themselves by hindering interlayer stress transfer [8–10]. Up to now, some methods were developed to flatten the sheet wrinkles by external force field in the solution state of the film, but the wrinkles are inevitably formed during the drying process [11]. Therefore, it is important to flatten the wrinkles in the dried films. Recently, a post-plasticization stretching method can achieve this goal in the pure graphene films [12]. However, it remains a challenge to decrease the random wrinkles in graphene-based composites to improve their final performances.

Here, we fabricated high performance nacre-like graphene-based composite materials by reducing the wrinkles of graphene via plasticization stretching strategy. The achieved graphene-polyvinyl alcohol (PVA) composite film owns tensile strength of 709.2 MPa and toughness of 11.1 MJ m^{-3}, which are 193% of the strength (366.7 MPa) and 158% of the toughness (6.9 MJ m^{-3}) of direct-cast graphene-PVA composite film. The strength and toughness also far exceed those nature nacre (80–135 MPa, 0.2–1.8 MJ m^{-3}). Besides, the electrical conductivity of the composite film is 7671 S m^{-1}, which is greatly improved compared to the other graphene-polymer composite materials. This facile plasticization stretching method is applicable to other 2D nanosheets to create high-performance composites.

2. Experimental

The experimental details can be referred in Supporting Information.

* Corresponding author.
** Corresponding author.
E-mail addresses: yingjunliu@zju.edu.cn (Y. Liu), chaogao@zju.edu.cn (C. Gao).

https://doi.org/10.1016/j.coco.2021.100815
Received 11 April 2021; Received in revised form 24 May 2021; Accepted 26 May 2021
Available online 2 June 2021

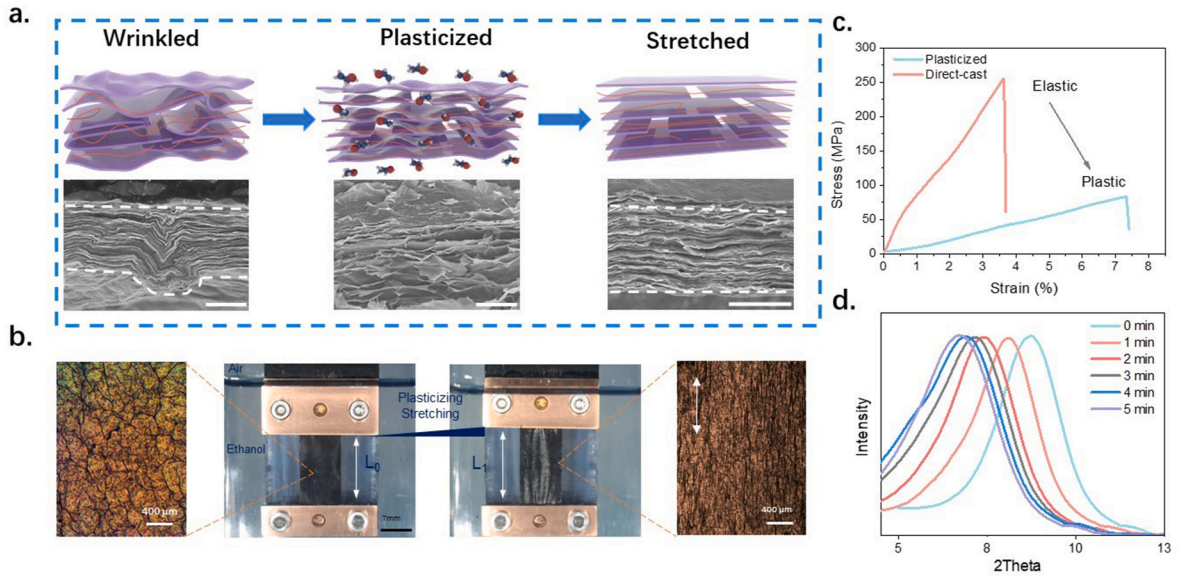

Fig. 1. a) Schematic structures of wrinkled, plasticized and stretched GO-PVA films and corresponding SEM images. b) Plasticization and stretching process of GO-PVA film. c) Typical stress-strain curves of the plasticized and the direct-cast GO-PVA films. d) XRD patterns of GO-PVA films immersed in ethanol for different time. Scale bars, a 5 μm; b 400 μm.

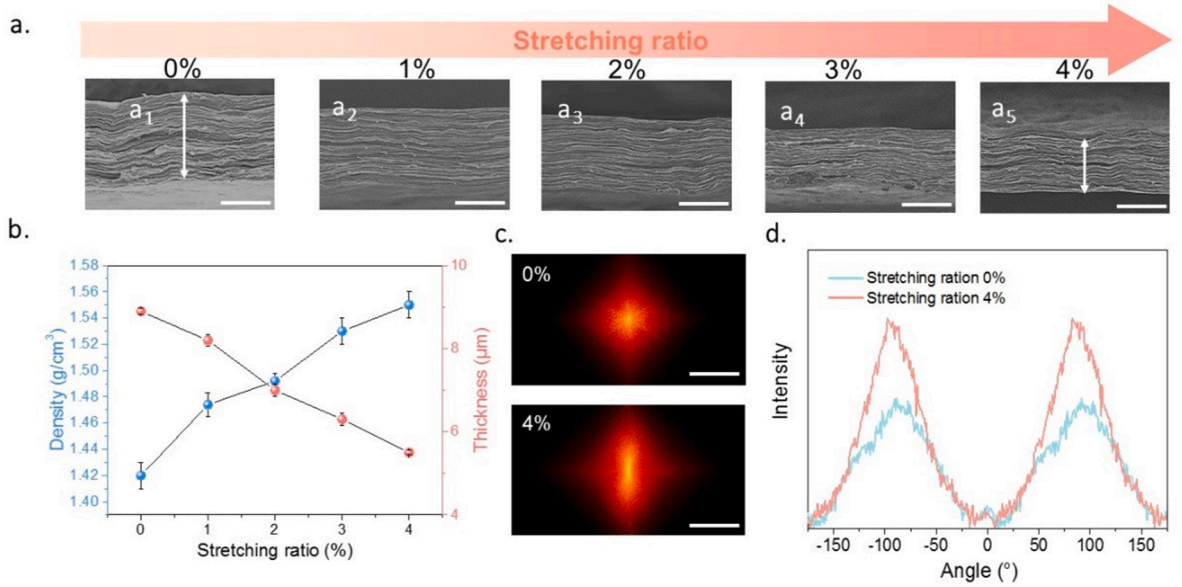

Fig. 2. a) SEM images of rGO films at different stretching ratio. b) Density and thickness of rGO-PVA films. c) FFT diffraction patterns of rGO-PVA films at 0% and 4% stretching ratio. d) Azimuth integral curves of Fig. 2c. Scale bars, 5 μm.

3. Results and discussion

3.1. Structure analysis of graphene-PVA composite film

The plasticization and stretching process of graphene-PVA composite film is shown in Fig. 1. The direct-cast graphene-PVA composite film features large wrinkles from the cross-sectional scanning electron microscope (SEM) image, which consists with previous reports [13–15]. To reduce these wrinkles, the composite film was completely immersed in ethanol that acts as a plasticizer (Fig. 1a), followed by continuously stretching. We traced the stretching process by optical microscope. The direct-cast film was riddled with numerous random wrinkles on the surface. While after plasticization and stretching, most of the random wrinkles are depressed, and we observed clear micro orientation along the stretching direction (Fig. 1b). When ethanol fully diffuses into the interlayer spacing of GO sheets, the film transits into a plastic state. This obvious transition could be verified by its mechanical behavior, as shown in the stress-strain curves (Fig. 1c). In particular, the breakage elongation of the plasticized GO-PVA film is 104% higher than that of direct-cast film (3.62%). We investigated the origin of this elastic-plastic transition through tracing the peak changes of X-ray diffraction (XRD) patterns. As shown in Fig. 1d, the interlayer spacing of GO sheets in the composite film gradually increases from 1.01 nm to 1.31 nm, because these intercalated small molecules could weaken the interaction of van der Waals between GO sheets [16]. Hence, GO sheets are activated to slide relatively under external tension. During this plasticization stretching process, the weak interlayer links (for example, hydrogen bonding) are fractured and reconstructed in balance, resulting in a

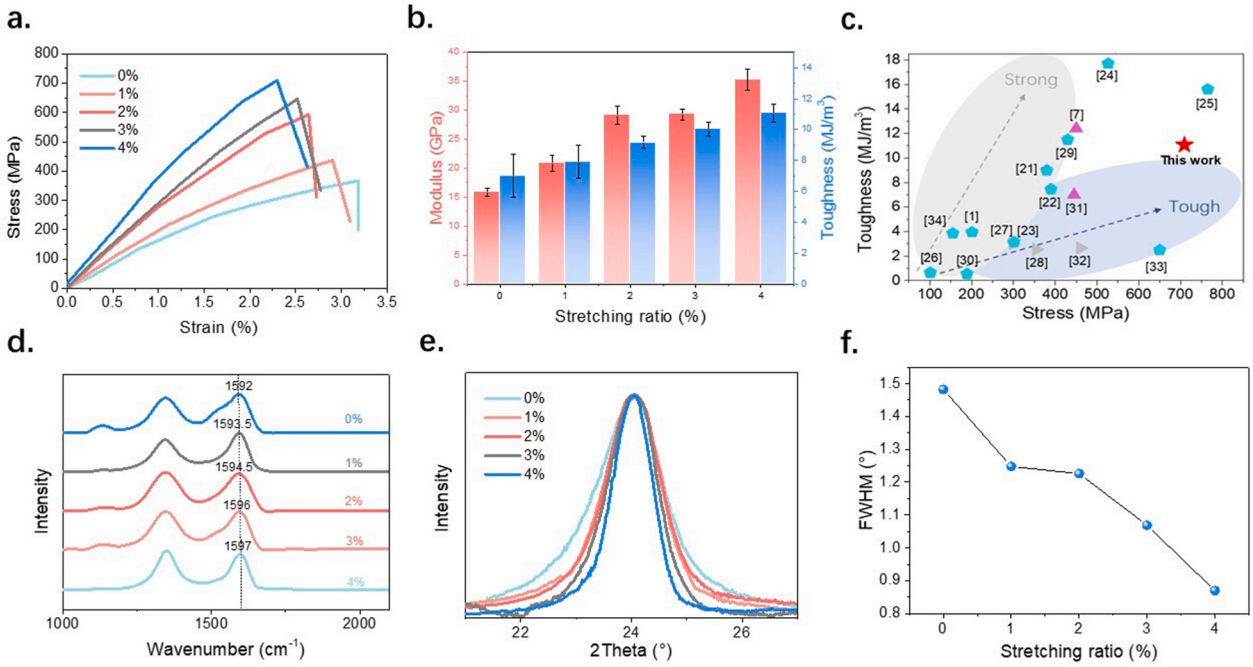

Fig. 3. a) Stress-strain curves and b) Toughness and Young's modulus of rGO-PVA films. c) Comparison of strength and toughness of 4%-rGO-PVA films with other reported rGO composites. The blue pentagon represents the composite film prepared by the mix of multiphase method, the purple triangle represents the composite film prepared by the LBL method, and the gray triangle represents the composite film prepared by the chemical grafting method. d) Raman spectra and e) XRD patterns of rGO-PVA films. f) FWHM of (002) peak in (e). (For interpretation of the references to colour in this figure legend, the reader is referred to the Web version of this article.)

dissipation of huge energy and an improvement of the breakage elongation [17,18].

The microstructure change of graphene-PVA composite film at different stretching ratios was analyzed by SEM. As shown in Fig. 2a, the GO sheet in the direct-cast film are stacked in a bent state. Subsequently, with the increment of the stretching ratio from 1% to 4%, the wrinkles of GO sheets gradually disappear with the thickness of the composite film decreases from 8.9 to 5.5 μm, which reduced by 61.8% of the original thickness (Fig. 2b). Simultaneously, the density increases from 1.42 to 1.55 g cm^{-3}. We analyze the orientation before (Fig. 2a_1) and after plasticization stretching (4%), respectively (Fig. 2a_5). Compared to direct-cast film (Fig. 2c, above), the beam in the Fast Fourier Transform (FFT) of the stretched film (Fig. 2c, below) is more concentrated. From the azimuth integral curves, the integrated area of stretched film is larger than the unstretched one, indicating that the graphene sheets become more regular and possess better orientation.

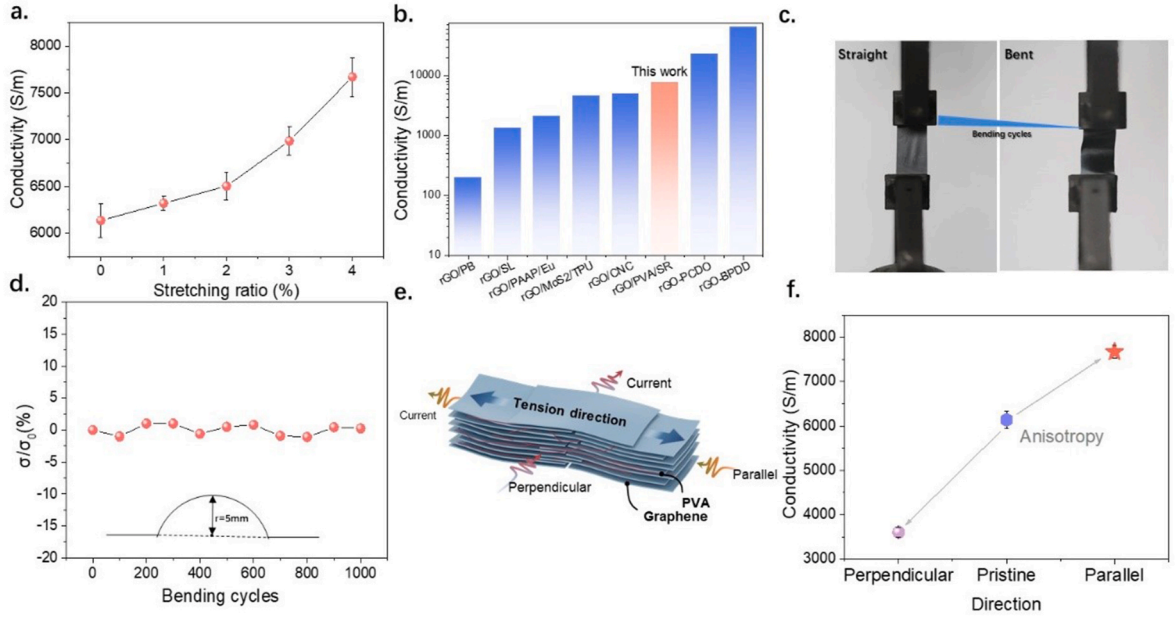

Fig. 4. a) Electrical conductivity of rGO composites. b) Comparison of conductivity of 4% stretching rGO-PVA film with other rGO composites. c) Photographs of the rGO-PVA film in straight and bent states. d) Conductivity variation under cyclic bending. e) Schematic of the conductivity tests. f) Comparison of conductivity in parallel and perpendicular to the direction of plasticization stretching.

Furthermore, the PVA also can be stretched along with GO during the plasticizing and stretching process because of the hydrogen bonds formed between the hydroxyl groups in PVA and the oxygen-containing functional groups of GO [19,20]. This phenomenon was confirmed by differential scanning calorimetry (DSC) tests (Supplementary Fig. 1). The relative glass transition temperature of PVA gradually increases from 31.7 to 38.7 °C, suggesting an increased crystalline process after stretching. Both the dewrinkled structure of graphene sheets and increased crystallinity of PVA may lead to enhanced mechanical performance.

3.2. The performances of graphene-PVA composite film

After plasticization and stretching, the mechanical properties of graphene-PVA composite film exhibited overall improvement along the uniaxial stretching direction. The strength of original film is 366.73 MPa. When the stretching ratio is 4%, the strength along the uniaxial stretching direction increases by 94%, reaching 709.23 MPa. The Young's modulus and toughness also gradually increase to 35.3 GPa and 11.06 MJ m^{-3}, showing a 122% and 58% improvement, respectively (Fig. 3b). Compared these properties with the composites obtained by other methods [1,7,21–34], our graphene-PVA composite film shows a high value in both toughness and strength (Fig. 3c). The value in perpendicular orientation is only 265 MPa (supplementary Figure.2), 71.8% of the pristine film. This can be ascribed to the existence of the wrinkles parallel to the uniaxial stretching direction after the plasticization and stretching process [12].

The mechanism for improvement of mechanical properties is investigated by Raman and XRD. With increment of stretching ratio, G peak shows a right shift from 1592 cm^{-1} to 1597 cm^{-1} (Fig. 3d). This phenomenon can be ascribed to the reduction of internal stress caused by wrinkled graphene during the stretching process [35,36]. From the XRD patterns (Fig. 3e), the interlayer spacing between GO sheets decreases from 0.485 to 0.481 nm after stretching for 4%. Moreover, the full-width at half-maximum (FWHM) shown in Fig. 3f gradually decreases from 1.482° to 0.870° during the stretching process, demonstrating an ordered orientation of graphene sheets and an enhanced crystallinity [37].

We further evaluate the conductivity change after stretching process. Benefiting from the better crystallinity, the electrical conductivity increases with the enhancement of stretching ratio (Fig. 4a). Compared with the conductivity of pristine film (6137 S m^{-1}), the conductivity reaches 7671 S m^{-1} after stretching, showing an improvement of 25%. This can be ascribed to the decreased wrinkles on graphene sheets and enhanced crystallinity of the film after plasticization and stretching process. Compared with previous work, the conductivity of our film is higher than that of majority of other composite films (Fig. 4b) [15,34,38–42]. Meanwhile, the electrical conductivity remains stable after 1000 bending tests (bending radius: 5 mm), suggesting the good bending resistance and structural stability (Fig. 4d). Moreover, the conductivity of the uniaxial stretched films exhibits high anisotropy. The conductivity in parallel orientation is 7671 S m^{-1} while the value in perpendicular orientation is 3605 S m^{-1} (Fig. 4e and f). The wrinkles in perpendicular orientation of plasticization stretching are mostly flattened after the plasticization stretching, which makes it easier for the transportation of electrons along the uniaxial stretching direction (Supplementary Fig. 3). However, wrinkles in parallel orientation still exist. So, the conductivity along the uniaxial stretching direction in the film (7671 S m^{-1}) is higher than that in perpendicular orientation of plasticization stretching (3605 S m^{-1}) [43].

4. Conclusion

We develop a facile post-processing strategy to fabricate high performance nacre-like graphene-PVA composite films by a simple plasticization stretching process. The solid composites are plasticized by small molecular solvents. The wrinkles on graphene sheets are gradually flattened under continuous stretching, facilitating formation of highly oriented and crystalline structure. The achieved composite film shows both excellent mechanical properties and high electrical conductivity. This highly efficient post-processing method promises an opportunity to construct 2D nanosheet based composites with superior properties in the industry scale.

CRediT authorship contribution statement

Cheng Sun: Writing – original draft, Methodology. **Peng Li:** Methodology. **Haoguang Huang:** Investigation. **Xin Ming:** Formal analysis. **Mincheng Yang:** Formal analysis. **Yingjun Liu:** Conceptualization, Supervision. **Chao Gao:** Supervision.

Declaration of competing interest

The authors declare that they have no known competing financial interests or personal relationships that could have appeared to influence the work reported in this paper.

Acknowledgements

This work is supported by the National Key R&D Program of China (No. 2016YFA0200200), National Natural Science Foundation of China (Nos. 52090030), Key Laboratory of Novel Adsorption and Separation Materials and Application Technology of Zhejiang Province (512301-I21502).

Appendix A. Supplementary data

Supplementary data to this article can be found online at https://doi.org/10.1016/j.coco.2021.100815.

References

[1] W. Cui, M. Li, L. Ji, B. Wang, C. Zhang, L. Jiang, Q. Cheng, A strong integrated strength and toughness artificial nacre based on dopamine cross-linked graphene oxide, ACS Nano 8 (2014) 9511–9517.
[2] V.B. Mohan, k. Lau, D. Hui, D. Bhattacharyya, Graphene-based materials and their composites: a review on production, applications and product limitations, Compos. B Eng. 142 (2018) 200–220.
[3] A.A. Balandin, S. Ghosh, W. Bao, I. Calizo, D. Teweldebrhan, F. Miao, C. Lau, Superior thermal conductivity of single-layer graphene, Nano Lett. 8 (2008) 902–907.
[4] A.H. Castro Neto, F. Guinea, N.M.R. Peres, K.S. Novoselov, A.K. Geim, The electronic properties of graphene, Rev. Mod. Phys. 81 (2009) 109–162.
[5] C. Huang, C. Cheng, Learning from nacre: constructing polymer nanocomposites, Compos. Sci. Technol. 150 (2017) 141–166.
[6] J. Peng, Q. Cheng, High-performance nanocomposites inspired by nature, Adv. Colloid Interface Sci. 29 (2017) 1702959.
[7] Z. Liu, Z. Xu, X. Hu, C. Gao, Lyotropic liquid crystal of polyacrylonitrile-grafted graphene oxide and its assembled continuous strong nacre-mimetic fibers, Macromolecules 46 (2013) 6931–6941.
[8] A. Zandiatashbar, G.H. Lee, S.J. An, S. Lee, N. Mathew, M. Terrones, T. Hayashi, C. R. Picu, J. Hone, N. Koratkar, Effect of defects on the intrinsic strength and stiffness of graphene, Nat. Commun. 5 (2014) 3186.
[9] Z. Qin, M. Taylor, M. Hwang, K. Bertoldi, M.J. Buehler, Effect of wrinkles on the surface area of graphene: toward the design of nanoelectronics, Nano Lett. 14 (2014) 6520–6525.
[10] K. Min, N.R. Aluru, Mechanical properties of graphene under shear deformation, Appl. Phys. Lett. 98 (2011), 013113.
[11] S. Liu, J. Liu, Z. Xu, Y. Liu, P. Li, F. Guo, F. Wang, Y. Liu, M. Yang, W. Gao, C. Gao, Artificial bicontinuous laminate synergistically reinforces and toughens dilute graphene composites, ACS Nano 12 (2018) 11236–11243.
[12] P. Li, M. Yang, Y. Liu, H. Qin, J. Liu, Z. Xu, Y. Liu, F. Meng, J. Lin, F. Wang, C. Gao, Continuous crystalline graphene papers with gigapascal strength by intercalation modulated plasticization, Nat. Commun. 11 (2020) 2645.
[13] S. Wan, Y. Chen, S. Fang, S. Wang, Z. Xu, L. Jiang, R.H. Baughman, Q. Cheng, High-strength scalable graphene sheets by freezing stretch-induced alignment, Nat. Mater. 20 (2021) 624–631.
[14] P. Li, Yi Liu, S. Shi, Z. Xu, W. Ma, Z. Wang, S. Liu, C. Gao, Highly crystalline graphene fibers with superior strength and conductivities by plasticization spinning, Adv. Funct. Mater. 30 (2020) 2006584.

[15] S. Ye, B. Chen, D. Hu, C. Liu, J. Feng, Graphene-based films with integrated strength and toughness via a novel two-step method combining gel casting and surface crosslinking, Chem. Nanomater. Energy 2 (2016) 816–821.
[16] C. Zhang, Y. Fujii, K. Tanaka, Effect of long range interactions on the glass transition temperature of thin polystyrene films, ACS Macro Lett. 1 (2012) 1317–1320.
[17] Y. Liu, B. Xie, Z. Zhang, Q. Zheng, Z. Xu, Mechanical properties of graphene papers, J. Mech. Phys. Solid. 60 (2012) 591–605.
[18] Y. Liu, Z. Xu, Multimodal and self-healable interfaces enable strong and tough graphene-derived materials, J. Mech. Phys. Solid. 70 (2014) 30–41.
[19] L. Yang, W. Weng, X. Fei, L. Pan, X. Li, W. Xu, Z. Hu, M. Zhu, Revealing the interrelation between hydrogen bonds and interfaces in graphene/PVA composites towards highly electrical conductivity, Chem. Eng. J. 383 (2020) 123–126.
[20] L. Shao, J. Li, Y. Guang, Y. Zhang, H. Zhang, X. Che, Y. Wang, PVA/polyethyleneimine-functionalized graphene composites with optimized properties, Mater. Des. 99 (2016) 235–242.
[21] S. Wan, H. Hu, J. Peng, Y. Li, Y. Fan, L. Jiang, Q. Cheng, Nacre-inspired integrated strong and tough reduced graphene oxide-poly(acrylic acid) nanocomposites, Nanoscale 8 (2016) 5649–5656.
[22] M. Zhang, L. Huang, J. Chen, C. Li, G. Shi, Ultratough, ultrastrong, and highly conductive graphene films with arbitrary sizes, Adv. Mater. 26 (2014) 7588–7592.
[23] X. Zhao, Z. Xu, B. Zheng, C. Gao, Macroscopic assembled, ultrastrong and H2SO4-resistant fibres of polymer-grafted graphene oxide, Sci. Rep. 3 (2013) 3164.
[24] S. Wan, J. Peng, Y. Li, H. Hu, L. Jiang, Q. Cheng, Use of synergistic interactions to fabricate strong, tough, and conductive artificial nacre based on graphene oxide and chitosan, ACS Nano 9 (1900) 9830–9836.
[25] Y. Wen, M. Wu, M. Zhang, C. Li, G. Shi, Topological design of ultrastrong and highly conductive graphene films, Adv. Mater. 29 (2017) 1702831.
[26] S. Park, K.S. Lee, G. Bozoklu, W. Cai, S.T. Nguyen, R.S. Ruoff, Graphene oxide papers modified by divalent ions—enhancing mechanical properties via chemical cross-linking, ACS Nano 2 (2008) 572–578.
[27] D.D. Kulkarni, I. Choi, S.S. Singamaneni, V.V. Tsukruk, Graphene oxide−Polyelectrolyte nanomembranes, ACS Nano 4 (2010) 4667–4676.
[28] P. Chammingkwan, K. Matsushita, T. Taniike, M. Terano, Enhancement in mechanical and electrical properties of polypropylene using graphene oxide grafted with end-functionalized polypropylene, Materials 9 (2016) 240.
[29] Y. Gao, H. Xu, Q. Cheng, Multiple synergistic toughening graphene nanocomposites through cadmium ions and cellulose nanocrystals, Adv. Mater. Interfaces 5 (2018) 1800145.
[30] K.W. Putz, O.C. Compton, M.J. Palmeri, S.T. Nguyen, L.C. Brinson, High-nanofiller-content graphene oxide-polymer nanocomposites via vacuum-assisted self-assembly, Adv. Funct. Mater. 20 (2010) 3322–3329.
[31] R. Xiong, H. Kim, L. Zhang, V.F. Korolovych, S. Zhang, Y.G. Yingling, V.V. Tsukruk, Wrapping nanocellulose nets around graphene oxide sheets, Angew. Chem. 57 (2018) 8508–8513.
[32] Y. Wang, R. Ma, K. Hu, S. Kim, G. Fang, Z. Shao, V.V. Tsukruk, Dramatic enhancement of graphene oxide/silk nanocomposite membranes: increasing toughness, strength, and Young's modulus via annealing of interfacial structures, ACS Appl. Mater. Interfaces 8 (2016) 24962–24973.
[33] E. Katz, Application of bifunctional reagents for immobilization of proteins on a carbon electrode surface: oriented immobilization of photosynthetic reaction centers, J. Electroanal. Chem. Interfacial Electrochem. 365 (1994) 157–164.
[34] Q. Cheng, M. Wu, M. Li, L. Jiang, Z. Tang, Ultratough artificial nacre based on conjugated cross-linked graphene oxide, Angew. Chem. 52 (2013) 3750–3755.
[35] C. Vallés, D.G. Papageorgiou, F. Lin, Z. Li, B.F. Spencer, R.J. Young, I.A. Kinloch, PMMA-grafted graphene nanoplatelets to reinforce the mechanical and thermal properties of PMMA composites, Carbon 157 (2020) 750–760.
[36] F. Wang, I.A. Kinloch, D. Wolverson, R. Tenne, A. Zak, E. O'Connell, U. Bangert, R. J. Young, Strain-induced phonon shifts in tungsten disulfide nanoplatelets and nanotubes, 2D Mater. 4 (2016) 15007.
[37] A. Oberlin, M. Oberlin, Graphitizability of carbonaceous materials as studied by TEM and X-ray diffraction, J. Microsc. 132 (1983) 353–363.
[38] S. Wan, Y. Chen, Y. Wang, G. Li, G. Wang, L. Liu, J. Zhang, Y. Liu, Z. Xu, A. P. Tomsia, L. Jiang, Q. Cheng, Ultrastrong graphene films via long-chain π-bridging, Matter 1 (2019) 389–401.
[39] S. Keten, M.J. Buehler, Geometric confinement governs the rupture strength of H-bond assemblies at a critical length scale, Nano Lett. 8 (2008) 743–748.
[40] S. Wan, Y. Li, J. Peng, H. Hu, Q. Cheng, L. Jiang, Synergistic toughening of graphene oxide–molybdenum disulfide–thermoplastic polyurethane ternary artificial nacre, ACS Nano 9 (2015) 708–714.
[41] Y. Xu, H. Bai, G. Lu, C. Li, G. Shi, Flexible graphene films via the filtration of water-soluble noncovalent functionalized graphene sheets, J. Am. Chem. Soc. 130 (2008) 5856–5857.
[42] K. Hu, L.S. Tolentino, D.D. Kulkarni, C. Ye, S. Kumar, V.V. Tsukruk, Written-in conductive patterns on robust graphene oxide biopaper by electrochemical microstamping, Angew. Chem. 52 (2013) 13784–13788.
[43] J. Lin, P. Li, Y. Liu, Z. Wang, Y. Wang, X. Ming, C. Gao, Z. Xu, The origin of the sheet size predicament in graphene macroscopic papers, ACS Nano 15 (2021) 4824–4832.